The metabolic abnormalities of chronic high dose glucocorticoids are not mediated by hypothalamic AgRP in male mice

Charlotte Sefton[1], Alison Davies[1], Tiffany-Jayne Allen[1], Jonathan R Wray[1], Rosemary Shoop[1], Antony Adamson[2], Neil Humphreys[2,4], Anthony P Coll[3*], Anne White[1*] & Erika Harno[1*]

1. Division of Diabetes, Endocrinology and Gastroenterology, Faculty of Biology, Medicine and Health, University of Manchester, Manchester Academic Health Sciences Centre, Manchester, M13 9PT, UK.
2. Manchester Transgenic Unit, University of Manchester, Manchester Academic Health Sciences Centre, Manchester, M13 9PT, UK.
3. University of Cambridge Metabolic Research Laboratories and MRC Metabolic Diseases Unit, Wellcome-MRC Institute of Metabolic Science, Addenbrooke's Hospital, Cambridge, CB2 0QQ, UK.
4. Current address: Gene Editing and Embryology Facility, EMBL Monterotondo, Rome, Italy.
* joint last authors

Short title: AgRP doesn't mediate Gc-induced metabolic effects

Key Words (six max): Glucocorticoids, Obesity, Diabetes, Hypothalamus, AgRP

Correspondence and reprint requests to:

Dr E. Harno,

Division of Diabetes, Endocrinology and Gastroenterology,

School of Medical Sciences,

Faculty of Biology, Medicine and Health, University of Manchester,

Manchester Academic Health Sciences Centre,

3.020 AV Hill Building,

Manchester,

M13 9PT,

UK.

Tel.: +44 (0) 161 306 6041

E-mail address: erika.harno@manchester.ac.uk

Professor A. White,

Division of Diabetes, Endocrinology and Gastroenterology,

School of Medical Sciences,

Faculty of Biology, Medicine and Health, University of Manchester,

Manchester Academic Health Sciences Centre,

3.016 AV Hill Building,

Manchester,

M13 9PT,

UK.

Tel.: +44 (0) 161 275 5178

E-mail address: anne.white@manchester.ac.uk

Dr A.P. Coll

University of Cambridge Metabolic Research Laboratories and MRC Metabolic Diseases Unit,

Wellcome-MRC Institute of Metabolic Science,

Addenbrooke's Hospital,

Cambridge, CB2 0QQ,

UK.

Tel +44 (0) 1223 769041

E-mail address: apc36@cam.ac.uk

Grants/fellowships:

This study was supported by the Mawer-Fitzgerald Endowment Fund at the University of Manchester. APC is supported by the Medical Research Council (MRC Metabolic Diseases Unit [MRC_MC_UU_12012.1]).

The authors report no conflict of interests.

Abstract

Glucocorticoids (Gcs) are potent and widely used medicines, but often cause metabolic side effects. A murine model of corticosterone (Cort) treatment results in increased hypothalamic expression of the melanocortin antagonist AgRP in parallel with obesity and hyperglycaemia. This study investigates how these adverse effects develop over time with particular emphasis on hypothalamic involvement.

Wild type and *Agrp*$^{-/-}$ male mice were treated with Cort for three weeks. Phenotypic, biochemical, protein and mRNA analysis was undertaken on central and peripheral tissues including white and brown adipose tissue, liver and muscle to determine the metabolic consequences.

Cort treatment induced hyperphagia within one day in wild type mice and this persisted for three weeks. Despite this early increase in food intake, body weight only started to rise after ten days. Hyperinsulinaemia occurred at day one, and although after two days there were alterations in genes often associated with insulin resistance in several peripheral tissues, hyperglycaemia only developed at three weeks. Throughout there was a sustained elevation in hypothalamic *Agrp* expression. Mice with *Agrp* deleted (using CRISPR-Cas9, *Agrp*$^{-/-}$) were partially protected against Cort-induced hyperphagia. However, *Agrp*$^{-/-}$ mice still had similar Cort-induced increases in body weight and adiposity to *Agrp*$^{+/+}$ mice. Loss of AgRP did not diminish Cort-induced hyperinsulinaemia or correct changes in hepatic gluconeogenic genes.

Chronic Gc treatment in mice mimics many of the metabolic side effects seen in patients and leads to a robust increase in *Agrp*. However, AgRP does not appear to be responsible for the majority of the Gc-induced adverse metabolic effects.

Introduction:

Synthetic glucocorticoids (Gcs) are a widely used class of medicines, important in the treatment of numerous inflammatory disorders including rheumatoid arthritis and asthma, and regularly used after organ transplantation. In the short-term, they are generally well tolerated, however, longer-term administration can lead to a range of adverse effects including weight gain, hyperglycaemia, and osteoporosis. Although prophylactic treatment is often used to ameliorate skeletal side effects like osteoporosis, there are no specific interventions to mitigate the metabolic changes.

The mechanisms by which chronically increased Gcs give rise to these adverse metabolic profiles are complex. The increased incidence of obesity seen in patients with chronically elevated Gcs may derive from Gc-induced hyperphagia. This is seen in several rodent studies of chronic Gc treatment (1-3). The hypothalamus has a key role in appetitive behaviour and Gcs may drive this change in food intake by acting within this brain region. This is evidenced from Gc effects on a number of neuropeptides including POMC (4, 5), AgRP (6, 7), and NPY (4, 6, 8). However, the reported effects of Gcs on these energy-regulatory neuropeptides are often conflicting.

The actions of Gcs on peripheral tissues are complex. For example, in white adipose tissue (WAT) Gcs are known to be lipolytic (9), but can also cause fat redistibution, typically diminishing subcutaneous fat and increasing intra-abdominal obesity (10). Gcs can also affect brown adipose tissue (BAT), with a reduction in levels of UCP-1, an essential protein in non-shivering

thermogenesis, reported in multiple rodent models (11, 12). However, there appear to be species-specific differences in this response (13) and whether this potential suppression of BAT activity results in changes in energy expenditure sufficient to alter body fat stores in the longer term remains to be fully determined. Similarly, although there are well-described molecular mechanisms for the acute effects of Gcs on hepatic glucose output (14), it is less clear what effects chronic Gcs may have in the presence of prolonged hyperinsulinaemia and insulin resistance.

We have previously reported that mice administered corticosterone (Cort; 75μg/ml) in drinking water had increased hypothalamic corticosterone levels, which caused changes in Gc target genes and an elevation in the orexigenic neuropeptide AgRP after four weeks (3). There is increasing evidence that central molecular pathways, involving neuropeptides like AgRP, are able to signal from the hypothalamus to have specific metabolic effects on peripheral tissues including WAT (15), BAT (16) and liver (17). However, the evolution and the mechanisms driving Gc-induced metabolic effects remain unclear. Therefore, in the current study we have investigated how and when the different adverse effects of Gcs develop over time and used a mouse model of *Agrp* deficiency to determine the role of AgRP in their development. We found an immediate increase in food intake but a delayed increase in body weight and fat pad mass. Furthermore, although *Agrp* increased rapidly in parallel with elevated food intake, loss of *Agrp* did not protect from weight gain or hyperinsulinaemia.

Material and Methods:

Generation of AgRP$^{-/-}$ mice

To generate an AgRP KO transgenic mouse line (*Agrp*$^{-/-}$) we used Clustered Regularly Interspaced Short Palindromic Repeats (CRISPR)-Cas9 technology, and designed four sgRNA which flanked the entire protein coding sequences (Figure 1). Two sgRNA targeted upstream, and two targeted downstream of the gene, which in the event of combined cutting would result in the excision of the full gene. We also designed an ssDNA template to facilitate a precise HDR event. The sgRNA were selected using the Sanger WTSI website [http://www.sanger.ac.uk/htgt/wge/; (18)] using stringent criteria for off target predictions (guides with mismatch (MM) of 0, 1 or 2 for elsewhere in the genome were discounted. MM3 were tolerated if predicted off targets were not exonic).

We synthesised sgRNA using previously described protocols (19). Briefly, a forward oligonucleotide for each sgRNA was designed according to the template from CRISPR_F (replacing GGN18-20 with guide sequence) and 10μM forward primer combined with 10μM universal CRISPRsgR primer were used in a PCR reaction with high fidelity polymerase (Phusion, NEB, MA, USA). 200ng of the resulting amplicon were used as a template in an *in vitro* transcription reaction (HiScribe, NEB), before purification (Megaclear, Ambion, UK) and quantification by NanoDrop.

An injection mix of the four sgRNA (20ng/μl each) and Cas9 mRNA (100ng/μl) was prepared and directly microinjected into B6D2F1 (Envigo, UK) zygote pronuclei using standard protocols. Zygotes were cultured overnight and the

resulting two cell embryos surgically implanted into the oviduct of day 0.5 post-coitum pseudopregnant CD1 mice. Potential founder mice were screened by PCR, with genotyping primers F1:ctgccatataagctcagggca and R1:tggtgccttaaactcgccc. On a wild type template these primers amplify an 1100bp band, whereas excision of the gene results in band of ~200-300bp. We obtained several candidate mice (10/18), and took five forward for sequencing following PCR-Blunt cloning, and confirmed full loss of gene in each. Two founder mice (2 and 5, Figure 1) were identified and then back-crossed to C57Bl/6J wild type mice to assess germline penetrance with line 5 taken forward. Colonies were genotyped as above. The *Agrp*$^{-/-}$ mice produced offspring litters in Mendelian ratios and were maintained by intercrosses on the mixed C57Bl/6J and DBA/2J background.

Study Design

C57Bl/6J mice were purchased from Charles River (UK), and *Agrp*$^{-/-}$ mice and their *Agrp*$^{+/+}$ littermates were bred at the University of Manchester. All mice were maintained under a 12:12 light:dark cycle (lights on 07:00, lights off 19:00) in specific pathogen free cages with wood chip bedding and environmental enrichment. Food and water were available *ad libitum*.

Ten week old male mice were singly housed and acclimatised for one week, before a two week baseline, where body weight, food, and water intake were monitored daily (short studies) or twice weekly (three week studies). Mice were assigned to treatment groups of corticosterone (Sigma-Aldrich, UK; 75µg/ml in 1% ethanol, Cort, (3) or vehicle (1% ethanol) in drinking water, so that each

group had mice with equivalent baseline body weight and food intake. *Agrp*$^{-/-}$ and *Agrp*$^{+/+}$ mice were randomly assigned at genotyping. The dose of Cort was chosen based on a previous dose finding study, where lower doses of Cort were found not to give a full range of metabolic phenotypic effects. Mice were treated for one, two, or three days or three weeks and body weight, food, and water intake were measured as the baseline period. Upon veterinary advice, mice drinking >15ml/day of treatment were changed onto water during the day. This occurred for ~20% of the mice administered Cort for three weeks. At termination, mice were tail bled to measure glucose and insulin, prior to euthanasia by rising CO_2 followed by exsanguination. Tissues were weighed and then snap frozen (Qiagen, UK) or 10% formalin. Whole hypothalami were isolated for mRNA expression analysis, microdissection scissors were used to cut immediately caudal to the optic chiasm and dorsally by the mammillothalamic tract, the dissection was limited laterally by the hypothalamic sulci. The entire hypothalamus was then removed and placed in RNAlater prior to RNA extraction.

All experiments were carried out in accordance with the United Kingdom Home Office legislation (Animal (Scientific Procedures) Act 1986) and were approved by the local ethics committee, University of Manchester, UK. All experiments were performed in accordance with the relevant guidelines and regulations.

Biochemical measurements

Glucose was measured fresh in tail-prick blood samples using a glucometer (Accu-Chek, Roche, UK). For other analytes, blood was centrifuged, plasma

removed and stored at -80°C. Leptin (Millipore, UK) and insulin (CrystalChem, IL, USA) were measured by ELISA. For the homeostatic model assessment – insulin resistance (HOMA-IR), mice were fasted for 16h overnight prior to samples being taken (20).

Real-Time Quantitative PCR (qRT-PCR)

RNA was extracted using an RNeasy mini kit (Qiagen) with on column genomic DNA digestion according to the manufacturer's protocol, with an additional phenol extraction for adipose tissue. RNA was reverse transcribed (High Capacity cDNA RT, Applied Biosystems, UK) and transcript levels were determined on a Prism 7900HT (Applied Biosystems) with either TaqMan Gene Expression Assays and TaqMan Universal Master Mix II (Applied Biosystems) or SYBR assays designed with primer-BLAST software (NCBI, MD, USA) and GoTaq qPCR Master Mix (Promega, UK). Catalogue numbers and primer sequences are listed in Table 1. Samples were quantified using a standard curve with HPRT or TBP for TaqMan or SYBR assays respectively as housekeepers, and the vehicle group as calibrator.

Immunohistochemistry

Tissues were fixed in 10% formalin, 24h, and cryoprotected in 30% sucrose, 24h, frozen in OCT (Klinipath, Netherlands) using supercooled 2-methylbutane, and stored at -80°C. All tissues were cryosectioned at 12µm.

H&E staining

Frozen sections were rehydrated in a graded ethanol series (100%-70%), stained with Shandon Gills No. 2 haematoxylin and Shandon eosin Y (both Thermo Fisher), before dehydration in increasing ethanol concentrations (70%-100%). Sections were mounted in DPX medium (Sigma) and cover slipped. Images presented are representative of three sections per mouse and four mice per group.

Oil Red O staining

Sections were stained with Oil Red O (CI 26125, Sigma-Aldrich) (21), and counterstained with Shandon Gills No.2 haematoxylin.

Agrp in situ hybridisation

In situ hybridisation was performed on frozen brain sections, three per group (*Agrp*$^{-/-}$ and *Agrp*$^{+/+}$) as previously described (3). An anti-sense Digoxigenin labelled riboprobe was generated using a T7 *in vitro* transcription system (Promega,) in the presence of a Digoxigenin (DIG) labelling mix (Roche) and an RNA expression vector pGM-5ZF(+) vector (Promega) containing the *Agrp* cDNA sequence from 196-777bp of sequence NM_001271806.1_ (581bp).

The riboprobe was hybridised overnight, 60°C, then the sections were rinsed in 4x SSC (Promega) followed by 2µg/ml RNaseA (Sigma-Aldrich) in 10mM Tris pH8.0, 1mM EDTA, 0.5M NaCl. After a final wash in 0.5x SSC, 60°C, sections were blocked in 2% FCS and incubated with anti-DIG-AP antibody (1:1500, Roche (22)) overnight, 4°C. After washing, the signal was revealed by incubation in 2% NBT/BCIP solution (Roche) for 2h.

Imaging

All images were visualised using a 20x/0.80 Plan Apo objective using the 3D-Histech Pannoramic-250 Flash II slide-scanner (3D-Histech, Hungary). Snapshots of the slide-scans were taken using CaseViewer software (3D-Histech).

Western Blot

BAT was thawed in RIPA buffer (Sigma-Aldrich) supplemented with EDTA and protease inhibitors (Stratech, UK) before being homogenised (Qiagen). Protein concentration was estimated by Bradford assay (Bio-Rad, UK). Proteins were separated by SDS-PAGE (Thermo Fisher) and transferred to PVDF membrane. Membranes were blocked in Odyssey-PBS Blocking buffer (LI-COR Biosciences, UK) for 1h before incubating with primary antibodies [1:5000 anti-β-actin (Proteintech, UK; 60008-1-Ig; (23)), 1:1000 anti-UCP-1 (Abcam, UK; ab10983; (24))] diluted in TBS-T, overnight at 4°C. After washing in TBS-T, membranes were incubated with secondary antibodies (1:5000 800CW donkey anti-rabbit (926-32213; (25)) or 680RD goat anti-mouse (925-68070; (26)), both LI-COR Biosciences) prepared in TBS-T for 1h at RT. Membranes were visualised using an Odyssey CLx scanner and protein expression determined using Image Studio™ Lite Version 5.2 software (LI-COR Biosciences) with β-actin as the loading control.

Indirect Calorimetry

A comprehensive lab animal monitoring system (CLAMS, Columbus instruments, OH, USA) was used to measure metabolic gases, every 18min, in a separate

cohort of mice. Mice were acclimatised to cages for 24h, following which oxygen consumption (VO_2), carbon dioxide production (VCO_2) and respiratory exchange ratio (RER) were measured for a further 48h. Mice were then treated for a further 14 days. Energy expenditure was analysed by ANCOVA using body weight as a covariate (27) and as hourly averages normalised to body weight. RER data was plotted as hourly averages and was normalised to body weight. Mice in CLAMS cages showed identical phenotypic changes with Cort treatment compared with mice in home cages.

Statistical Analysis

Data were analysed using Prism 7.0 (GraphPad, CA, USA) and are presented as mean±S.E.M. For normally distributed data, Student's t-test was carried out between 2 groups. For qRT-PCR data, groups were compared using a Mann-Whitney test. A 2-way ANOVA was used for body weight and food intake data. ANCOVA analysis was carried out using SPSS (IBM, NY, USA). *P*-value of 0.05 was considered significant.

Results

Excess Gcs rapidly increase food intake, with a delayed gain in body weight and fat pad mass.

Food intake increased by 18% after one day of Cort treatment and was still elevated by three weeks (Figure 2a), with mice ingesting nearly 20% more each day. However, we did not observe a change in body weight during the first three days of Cort treatment (Figure 2b). Overall body weight did not start to differ

until day ten (data not shown) and was significantly increased by three weeks (Figure 2b).

There was a small increase in inguinal fat on day three, but by three weeks, inguinal, epididymal, and mesenteric fat pads had all at least doubled in mass (Figure 2c). This was accompanied by an increase in adipocyte size as shown in epididymal fat (Figure 2d). Additionally, gastrocnemius muscle weight was decreased after day two and three and there was also a trend towards a decrease in the mass of this tissue at three weeks (Figure 2e).

Circulating leptin levels were increased five-fold after day one of Cort treatment (Figure 2f), accompanied by at least a two-fold increase in *Lep* mRNA in white and brown adipose tissue (Figure 2g). At three weeks, there was a 65-fold elevation in leptin concentrations in plasma (Figure 2f) and a higher fold increase in *Lep* mRNA expression in inguinal (11.2-fold) and epididymal (4.8-fold) adipose tissue as well as in BAT (10.3-fold) (data not shown).

Cort increases BAT mass with no change in energy expenditure

BAT mass was increased with one day Cort treatment and this was maintained over the other time points (Figure 3a). This was associated with lipid infiltration into the tissue at two days, (Figure 3b). Additionally, there were changes in genes associated with thermogenesis in BAT after two days Cort treatment. *Cidea, Prdm16,* and *Ucp1* mRNA expression were decreased (Figure 3c) and at three weeks, *Ppargc1a* mRNA expression was also decreased (Figure 3e). UCP-1

protein levels were not reduced until four weeks (Figure 3d), when the lipid infiltration observed at day two remained (Figure 3b).

Energy expenditure was not changed by Cort treatment during either the light or dark phase in mice over days 1-3 or days 12-14 (data not shown). There was also no significant effect of Cort on energy expenditure after ANCOVA with body weight as a covariate (Figure 3f). However, in the Cort treated group there was a sustained elevation in respiratory exchange ratio (RER) during the light phase, in contrast to the fall in RER seen during light phase in the vehicle group (Figure 3g).

Cort treatment altered markers of insulin resistance

Circulating insulin was increased ten-fold after one day of Cort, with a further increase observed after three weeks treatment (Figure 4a). In light of this rapid and significant rise in circulating insulin, we looked at the expression of a number of well characterised genes that are recognised to correlate with insulin resistance. After only two days Cort treatment, there was a decrease in *Irs1* in skeletal muscle, liver, and epididymal fat tissue (Figure 4b). PI3-kinase subunit *P85α* mRNA expression increased in skeletal muscle, liver, BAT, and inguinal fat pads (data not shown). In BAT, the mRNA expression of another PI3-kinase subunit, *P110β*, was decreased (data not shown), indicating that there may be features of early insulin resistance in all the tissues examined.

After three weeks of chronic Cort, there were further changes in *Irs1, P85α* and *P110β* mRNA, in skeletal muscle, WAT and BAT in a manner associated with

399 insulin resistance (Figure 4c, data not shown). After three weeks of Cort, there
400 was clear hepatic steatosis which had not been present at two days (Figure 4d).
401 In liver, *Irs1* mRNA was decreased (Figure 4c) and *P85α* was increased (data not
402 shown). In keeping with systemic insulin resistance, after chronic Cort there was
403 a significant rise in HOMA-IR (Figure 4e).
404
405 Hyperglycaemia was not present during the early stages of Cort treatment but
406 had developed by three weeks in the Cort-treated mice (Figure 4f). Glucose 6-
407 Phosphate (*G6pc*), glucokinase (*Gck*), GLUT-2 (*Slc2a2*), Glycogen phosphorylase
408 (*Pygl*) expression in the liver were all unchanged by short-term Cort
409 administration (Figure 4g), but were increased after three weeks Cort treatment
410 (Figure 4h). PEPCK (*Pck1/2),* was not altered at either time (Figure 3g, 3h).
411
412 *Agrp expression is elevated with Cort treatment*
413 Central hypothalamic mechanisms have an important role in the control of
414 peripheral metabolism and we have previously shown that Cort can increase
415 *Agrp* after four weeks Cort treatment. However, in this study we have extended
416 our findings in groups of mice treated with Cort for one, two, and three days.
417 Cort induced an increase in *Agrp* expression after only one day and this was
418 sustained at days two and three (Figure 5a). Furthermore, *Agrp* was still
419 increased in the mice treatment with Cort for three weeks (Figure 5b). None of
420 the other genes analysed showed such a pronounced or persistent change in
421 expression (Figure 5a).
422
423 *Knockout of Agrp by CRISPR-Cas9*

To investigate whether the robust *Agrp* response to exogenous Cort was necessary for the development of the adverse effects observed, we studied the effect of Cort in a mouse engineered to lack *Agrp*. CRISPR-Cas9 was used to develop a novel *Agrp* null mouse ($Agrp^{-/-}$). *In situ* hybridisation confirmed loss of *Agrp* in $Agrp^{-/-}$ mice, compared to littermate controls ($Agrp^{+/+}$, Figure 6a). In addition, qRT-PCR confirmed the loss of *Agrp* in whole hypothalami from $Agrp^{-/-}$ mice (Figure 6b). As expected, *Agrp* was not detectable in Cort treated $Agrp^{-/-}$ mice.

Loss of Agrp partially protects male $Agrp^{-/-}$ mice from Cort-induced hyperphagia but does not protect against body weight gain

As previously, *Agrp* expression was increased in Cort-treated $Agrp^{+/+}$ mice (Figure 6b). Loss of *Agrp* partially protected mice against Cort-induced hyperphagia (Figure 6c). Analysis by two-way ANOVA indicated an interaction ($P<0.001$) between genotype and Cort treatment, making the data more difficult to interpret, therefore post hoc Tukey multiple comparison test was used and showed differences in Cort effect between Cort-$Agrp^{+/+}$ and Cort-$Agrp^{-/-}$ mice at days seven and ten. Cort induced a similar increase in food intake in $Agrp^{-/-}$ compared to their $Agrp^{+/+}$ littermates after day ten. To investigate whether other genes were driving the hyperphagia over this time period, we carried out mRNA analysis on a range of genes encoding neuropeptides and receptors involved in energy homeostasis. Loss of *Agrp* did not alter the basal expression of any of these genes (Figure 6d). Importantly, in the hypothalamus, Gc-responsive genes (*Fkbp5*, *Gilz*, *Nr3c1*, *Hsd11b1*) changed with Cort in both Cort-$Agrp^{-/-}$ mice and

448 Cort-*Agrp*$^{+/+}$ mice, indicating that Cort was acting similarly in the hypothalamus
449 of *Agrp*$^{-/-}$ and *Agrp*$^{+/+}$ mice (Figure 6e).
450
451 Both *Agrp*$^{+/+}$ and *Agrp*$^{-/-}$ mice have a similar magnitude of increase in body
452 weight with Cort treatment (Figure 6f). At the end of the study, BAT, epididymal,
453 mesenteric and inguinal fat, had increased to a similar extent in Cort-treated
454 *Agrp*$^{+/+}$ and *Agrp*$^{-/-}$ mice (Figure 6g).
455
456 *Agrp deletion does not protect from Cort-induced hepatic steatosis, insulin*
457 *resistance, or hyperglycaemia*
458 After three weeks Cort treatment, hyperinsulinaemia was present in both *Agrp*$^{+/+}$
459 and *Agrp*$^{-/-}$ mice (Figure 7a). In addition, quantification of a number of well
460 characterised hepatic insulin signalling genes (*Irs1*, *P85a,* and *P110b*), that are
461 recognised to correlate with insulin resistance, indicated that loss of *Agrp* did not
462 prevent the changes in these genes (Figure 7b). Liver mass increased in both
463 *Agrp*$^{+/+}$ and *Agrp*$^{-/-}$ mice with chronic Cort treatment (Figure 7c), and this was
464 due to increased lipid deposition (Figure 7d).
465
466 Hyperglycaemia developed in Cort-*Agrp*$^{+/+}$ mice after three weeks, and there was
467 a non-significant trend towards an increase in blood glucose levels in *Agrp*$^{-/-}$
468 (Figure 7e). In both *Agrp*$^{+/+}$ and *Agrp*$^{-/-}$ Cort treated mice there was evidence for
469 changes in genes involved in gluconeogenesis even in the fed state (Figure 7f).
470
471
472 **Discussion:**

473 This study of chronic Cort treatment in mice has identified a complex array of
474 metabolic changes which evolve over time and involve both peripheral and
475 central changes in pathways regulating energy balance. With Cort treatment,
476 there was a rapid increase in food intake, which was sustained over three weeks.
477 Cort caused an increase in body weight, although not until day ten, and this
478 change was not associated with altered energy expenditure. Cort also induced
479 hyperinsulinemia after one day, with early changes in expression of genes
480 associated with insulin resistance in several peripheral tissues. This
481 subsequently resulted in hyperglycaemia at three weeks.
482
483 This model of chronic Cort treatment supports and extends the results of other
484 elegant studies using similar approaches but giving higher doses of Cort (1, 28-
485 30), indicating that this is a reliable approach to address the different potential
486 mechanisms underlying Gc induced metabolic abnormalities. Mice given Cort,
487 when GR is knocked down in adipose tissue, have improved glucose tolerance
488 and insulin sensitivity (29). In other studies, mice given Cort when there is
489 deletion of *Hsd11b1* (the enzyme responsible for regeneration of corticosterone)
490 identified Gc regeneration in adipose tissue as a key factor in Cort-induced
491 hepatic steatosis and fatty acid excess (28). Using a different approach, Bowles *et*
492 *al.* found that endocannabinoid signalling in liver was necessary to mediate the
493 adverse effects of Cort on hepatic steatosis and dyslipidemia (30).
494
495 One of the most striking findings of the current study was the marked effect of
496 chronic Cort in increasing food intake and hypothalamic *Agrp* throughout the
497 time course, with no consistent change in any of the genes encoding signalling

498 molecules and receptors known to be involved in energy balance. The ability of
499 Gcs to increase AgRP expression is supported by our previous studies (3, 6).
500 Furthermore, there is considerable evidence that AgRP promotes hyperphagia
501 (31, 32) and therefore the rise in *Agrp* would be predicted to contribute to the
502 increase in food intake observed.
503
504 To test whether the AgRP neuropeptide mediated the Cort-induced hyperphagia,
505 we developed mice with ablation of the *Agrp* gene. When these mice were
506 treated with chronic Cort, there was an initial phase where food intake was not
507 increased compared to Cort treated wild type mice. However we did not observe
508 the expected protection from Cort-induced hyperphagia after day ten. This was
509 surprising given the markedly increased *Agrp* expression in wild type mice
510 treated with Cort, which was consistent over several groups of mice. However,
511 we acknowledge that other factors other than those we have analysed here may
512 be playing a part in Gc-induced hyperphagia.
513
514 Although food intake increased after one day Cort treatment, body weight did
515 not increase until day ten, which suggests that Cort may also be affecting energy
516 expenditure. Some of our data indicate that Cort treatment may be reducing the
517 metabolic activity of BAT, both in the early stages and at the end of the study.
518 Due to increased lipid deposition, BAT weight was increased from day one,
519 which has been previously reported to be indicative of less active BAT (33).
520 Furthermore with Cort treatment, in BAT the protein levels of UCP-1, as well as
521 the mRNA expression of *Prdm16, Ucp1, Cidea,* and *Ppargc,* all decreased. These
522 are all markers that support the possibility of decreased energy expenditure (34-

36). However, we were unable to identify any differences in energy expenditure between Cort and vehicle group, either before or after the body weight gain. Nevertheless, with Cort treatment we did observe a sustained elevation in RER during the inactive phase at both the earlier timepoint and at day 14, which potentially indicates a change in nutrient partitioning and decreased metabolism of lipids.

Gcs are known to act directly on BAT (37, 38). However, the effects of Gcs on BAT, in the current study, are similar to those seen in mice with antagonism of the MC4R by SHU9119, suggesting that Gc-induced AgRP antagonism of MC4R might be causing these similar effects. In studies by Kooijman *et al*. (39) using SHU9119, a decrease in melanocortin tone in the hypothalamus led to lipid infiltration and a rapid increase in BAT mass (39), a decrease in UCP-1 protein expression (39), an increase in RER (39) and decrease in energy expenditure (39). A second study using SHU9119 (40) to chronically blockade central melanocortin receptors did not report a change in energy expenditure (40) but did see an elevation in RER and reduced *Ucp1* expression in BAT. However, in our study, there was no difference in BAT weight between $Agrp^{+/+}$ and $Agrp^{-/-}$ mice treated with Cort, indicating that the elevation in AgRP with Gc treatment is not directly responsible for the elevation in BAT weight.

After one day Gc treatment, circulating insulin was increased and after two days there were changes in insulin signalling genes in skeletal muscle, WAT, liver, and BAT. Whether these changes are due to Gcs acting centrally or peripherally is unknown. Deletion of GR in adipose tissue in adult mice has highlighted its

548 importance in Gc-induced systemic insulin resistance (29). However, central
549 mechanisms have also been proposed to cause peripheral insulin resistance. One
550 mechanism includes AgRP neurons (16, 41), which also have a role in the control
551 of hepatic glucose production (17). However, in the present study, removal of
552 AgRP peptide did not reverse the hyperinsulinemia or the effects on insulin
553 signalling genes caused by chronic Cort. Furthermore, in the *Agrp*$^{-/-}$ mice, there
554 did not appear to be any protection from the Cort-induced changes observed in
555 hepatic gluconeogenic genes. Therefore AgRP is unlikely to mediate these Gc
556 effects, although the current study has only focussed on measurement of insulin
557 and genes previously shown to be modified in insulin resistant states.
558
559 The current study also demonstrated that Cort treatment induced
560 hyperglycaemia, with blood glucose levels elevated between days 17 and 21. In
561 the early phase (day two of Cort treatment) rapid induction of
562 hyperinsulinaemia likely prevented early development of hyperglycaemia. This
563 elevation in circulating insulin may also have counteracted the ability of Gcs to
564 directly affect expression of PEPCK or G6Pase in the liver (42). Additionally, we
565 observed elevated circulating leptin, which, through a central action, may have
566 diminished hepatic gluconeogenesis (43).
567
568 In conclusion, in this model of Gc treatment, there is an evolution of changing
569 metabolic abnormalities, which finally lead to the weight gain and
570 hyperglycaemia that characterise the metabolic adverse effects of Gc treatment
571 in humans. Our study has investigated whether chronic Cort treatment targets
572 hypothalamic pathways involved in energy balance. However, despite a large and

consistent increase in hypothalamic *Agrp*, it appears that this neuropeptide does not have a central role in Gc-mediated metabolic adverse events.

Acknowledgments

Thanks to Roger Meadows for help with microscopy and image analysis. We would also like to acknowledge the support of Peter Walker in the Histology Core Facility, and staff in the BSU, Faculty of Biology, Medicine and Health, University of Manchester.

This study was supported by the Mawer-Fitzgerald Endowment Fund at the University of Manchester. APC is supported by the Medical Research Council (MRC Metabolic Diseases Unit [MRC_MC_UU_12012.1]). The Bioimaging Facility microscopes were purchased with grants from BBSRC, Wellcome and the University of Manchester Strategic Fund.

References:

1. Karatsoreos IN, Bhagat SM, Bowles NP, Weil ZM, Pfaff DW and McEwen BS. Endocrine and physiological changes in response to chronic corticosterone: a potential model of the metabolic syndrome in mouse. *Endocrinology*. 2010;**151**(5):2117-2127.

2. Auvinen HE, Coomans CP, Boon MR, Romijn JA, Biermasz NR, Meijer OC, Havekes LM, Smit JW, Rensen PC and Pereira AM. Glucocorticoid excess induces long-lasting changes in body composition in male C57Bl/6J mice only with high-fat diet. *Physiol Rep*. 2013;**1**(5):e00103.

598 3. Sefton C, Harno E, Davies A, Small H, Allen TJ, Wray JR, Lawrence CB, Coll
599 AP and White A. Elevated Hypothalamic Glucocorticoid Levels Are Associated
600 With Obesity and Hyperphagia in Male Mice. *Endocrinology*. 2016;**157**(11):4257-
601 4265.
602 4. Savontaus E, Conwell IM and Wardlaw SL. Effects of adrenalectomy on
603 AGRP, POMC, NPY and CART gene expression in the basal hypothalamus of fed
604 and fasted rats. *Brain Res*. 2002;**958**(1):130-138.
605 5. Makimura H, Mizuno TM, Beasley J, Silverstein JH and Mobbs CV.
606 Adrenalectomy stimulates hypothalamic proopiomelanocortin expression but
607 does not correct diet-induced obesity. *BMC Physiol*. 2003;**3**:4.
608 6. Coll AP, Challis BG, Lopez M, Piper S, Yeo GS and O'Rahilly S.
609 Proopiomelanocortin-deficient mice are hypersensitive to the adverse metabolic
610 effects of glucocorticoids. *Diabetes*. 2005;**54**(8):2269-2276.
611 7. Goto M, Arima H, Watanabe M, Hayashi M, Banno R, Sato I, Nagasaki H and
612 Oiso Y. Ghrelin increases neuropeptide Y and agouti-related peptide gene
613 expression in the arcuate nucleus in rat hypothalamic organotypic cultures.
614 *Endocrinology*. 2006;**147**(11):5102-5109.
615 8. Yi CX, Foppen E, Abplanalp W, Gao Y, Alkemade A, la Fleur SE, Serlie MJ,
616 Fliers E, Buijs RM, Tschop MH and Kalsbeek A. Glucocorticoid signaling in the
617 arcuate nucleus modulates hepatic insulin sensitivity. *Diabetes*. 2012;**61**(2):339-
618 345.
619 9. Peckett AJ, Wright DC and Riddell MC. The effects of glucocorticoids on
620 adipose tissue lipid metabolism. *Metabolism*. 2011;**60**(11):1500-1510.
621 10. Mayo-Smith W, Hayes CW, Biller BM, Klibanski A, Rosenthal H and
622 Rosenthal DI. Body fat distribution measured with CT: correlations in healthy

623 subjects, patients with anorexia nervosa, and patients with Cushing syndrome.
624 *Radiology*. 1989;**170**(2):515-518.
625 11. Poggioli R, Ueta CB, Drigo RA, Castillo M, Fonseca TL and Bianco AC.
626 Dexamethasone reduces energy expenditure and increases susceptibility to diet-
627 induced obesity in mice. *Obesity (Silver Spring)*. 2013;**21**(9):E415-420.
628 12. Strack AM, Bradbury MJ and Dallman MF. Corticosterone decreases
629 nonshivering thermogenesis and increases lipid storage in brown adipose tissue.
630 *Am J Physiol*. 1995;**268**(1 Pt 2):R183-191.
631 13. Ramage LE, Akyol M, Fletcher AM, Forsythe J, Nixon M, Carter RN, van
632 Beek EJ, Morton NM, Walker BR and Stimson RH. Glucocorticoids Acutely
633 Increase Brown Adipose Tissue Activity in Humans, Revealing Species-Specific
634 Differences in UCP-1 Regulation. *Cell Metab*. 2016;**24**(1):130-141.
635 14. Pasieka AM and Rafacho A. Impact of Glucocorticoid Excess on Glucose
636 Tolerance: Clinical and Preclinical Evidence. *Metabolites*. 2016;**6**(3).
637 15. Ruan HB, Dietrich MO, Liu ZW, Zimmer MR, Li MD, Singh JP, Zhang K, Yin
638 R, Wu J, Horvath TL and Yang X. O-GlcNAc transferase enables AgRP neurons to
639 suppress browning of white fat. *Cell*. 2014;**159**(2):306-317.
640 16. Steculorum SM, Ruud J, Karakasilioti I, Backes H, Engstrom Ruud L,
641 Timper K, Hess ME, Tsaousidou E, Mauer J, Vogt MC, Paeger L, Bremser S, Klein
642 AC, Morgan DA, Frommolt P, Brinkkotter PT, Hammerschmidt P, Benzing T,
643 Rahmouni K, Wunderlich FT, Kloppenburg P and Bruning JC. AgRP Neurons
644 Control Systemic Insulin Sensitivity via Myostatin Expression in Brown Adipose
645 Tissue. *Cell*. 2016;**165**(1):125-138.
646 17. Konner AC, Janoschek R, Plum L, Jordan SD, Rother E, Ma X, Xu C, Enriori
647 P, Hampel B, Barsh GS, Kahn CR, Cowley MA, Ashcroft FM and Bruning JC. Insulin

action in AgRP-expressing neurons is required for suppression of hepatic glucose production. *Cell Metab*. 2007;**5**(6):438-449.

18. Hodgkins A, Farne A, Perera S, Grego T, Parry-Smith DJ, Skarnes WC and Iyer V. WGE: a CRISPR database for genome engineering. *Bioinformatics*. 2015;**31**(18):3078-3080.

19. Bassett AR, Tibbit C, Ponting CP and Liu JL. Highly efficient targeted mutagenesis of Drosophila with the CRISPR/Cas9 system. *Cell Rep*. 2013;**4**(1):220-228.

20. Beaudry JL, D'Souza A M, Teich T, Tsushima R and Riddell MC. Exogenous glucocorticoids and a high-fat diet cause severe hyperglycemia and hyperinsulinemia and limit islet glucose responsiveness in young male Sprague-Dawley rats. *Endocrinology*. 2013;**154**(9):3197-3208.

21. Mehlem A, Hagberg CE, Muhl L, Eriksson U and Falkevall A. Imaging of neutral lipids by oil red O for analyzing the metabolic status in health and disease. *Nat Protoc*. 2013;**8**(6):1149-1154.

22. RRID:AB_2313640 https://scicrunch.org/resolver/AB_2313640

23. RRID:AB_2223182, https://scicrunch.org/resolver/AB_2223182

24. RRID:AB_2241462, https://scicrunch.org/resolver/AB_2241462

25. RRID:AB_621848, https://scicrunch.org/resolver/AB_621848

26. RRID:AB_2651128, https://scicrunch.org/resolver/AB_2651128

27. Tschop MH, Speakman JR, Arch JR, Auwerx J, Bruning JC, Chan L, Eckel RH, Farese RV, Jr., Galgani JE, Hambly C, Herman MA, Horvath TL, Kahn BB, Kozma SC, Maratos-Flier E, Muller TD, Munzberg H, Pfluger PT, Plum L, Reitman ML, Rahmouni K, Shulman GI, Thomas G, Kahn CR and Ravussin E. A guide to analysis of mouse energy metabolism. *Nat Methods*. 2011;**9**(1):57-63.

673 28. Morgan SA, McCabe EL, Gathercole LL, Hassan-Smith ZK, Larner DP,
674 Bujalska IJ, Stewart PM, Tomlinson JW and Lavery GG. 11beta-HSD1 is the major
675 regulator of the tissue-specific effects of circulating glucocorticoid excess. *Proc*
676 *Natl Acad Sci U S A*. 2014;**111**(24):E2482-2491.
677 29. Dalle H, Garcia M, Antoine B, Boehm V, Do TTH, Buyse M, Ledent T,
678 Lamaziere A, Magnan C, Postic C, Denis RG, Luquet S, Feve B and Moldes M.
679 Adipocyte Glucocorticoid Receptor Deficiency Promotes Adipose Tissue
680 Expandability and Improves the Metabolic Profile Under Corticosterone
681 Exposure. *Diabetes*. 2019;**68**(2):305-317.
682 30. Bowles NP, Karatsoreos IN, Li X, Vemuri VK, Wood JA, Li Z, Tamashiro KL,
683 Schwartz GJ, Makriyannis AM, Kunos G, Hillard CJ, McEwen BS and Hill MN. A
684 peripheral endocannabinoid mechanism contributes to glucocorticoid-mediated
685 metabolic syndrome. *Proc Natl Acad Sci U S A*. 2015;**112**(1):285-290.
686 31. Small CJ, Liu YL, Stanley SA, Connoley IP, Kennedy A, Stock MJ and Bloom
687 SR. Chronic CNS administration of Agouti-related protein (Agrp) reduces energy
688 expenditure. *Int J Obes Relat Metab Disord*. 2003;**27**(4):530-533.
689 32. Krashes MJ, Shah BP, Koda S and Lowell BB. Rapid versus delayed
690 stimulation of feeding by the endogenously released AgRP neuron mediators
691 GABA, NPY, and AgRP. *Cell Metab*. 2013;**18**(4):588-595.
692 33. Fischer AW, Hoefig CS, Abreu-Vieira G, de Jong JM, Petrovic N, Mittag J,
693 Cannon B and Nedergaard J. Leptin Raises Defended Body Temperature without
694 Activating Thermogenesis. *Cell Rep*. 2016;**14**(7):1621-1631.
695 34. van den Beukel JC, Boon MR, Steenbergen J, Rensen PC, Meijer OC,
696 Themmen AP and Grefhorst A. Cold Exposure Partially Corrects Disturbances in

Lipid Metabolism in a Male Mouse Model of Glucocorticoid Excess. *Endocrinology*. 2015;**156**(11):4115-4128.

35. Tan CY, Virtue S, Bidault G, Dale M, Hagen R, Griffin JL and Vidal-Puig A. Brown Adipose Tissue Thermogenic Capacity Is Regulated by Elovl6. *Cell Rep*. 2015;**13**(10):2039-2047.

36. Andrade JM, Frade AC, Guimaraes JB, Freitas KM, Lopes MT, Guimaraes AL, de Paula AM, Coimbra CC and Santos SH. Resveratrol increases brown adipose tissue thermogenesis markers by increasing SIRT1 and energy expenditure and decreasing fat accumulation in adipose tissue of mice fed a standard diet. *Eur J Nutr*. 2014;**53**(7):1503-1510.

37. Barclay JL, Agada H, Jang C, Ward M, Wetzig N and Ho KK. Effects of glucocorticoids on human brown adipocytes. *J Endocrinol*. 2015;**224**(2):139-147.

38. Soumano K, Desbiens S, Rabelo R, Bakopanos E, Camirand A and Silva JE. Glucocorticoids inhibit the transcriptional response of the uncoupling protein-1 gene to adrenergic stimulation in a brown adipose cell line. *Mol Cell Endocrinol*. 2000;**165**(1-2):7-15.

39. Kooijman S, Boon MR, Parlevliet ET, Geerling JJ, van de Pol V, Romijn JA, Havekes LM, Meurs I and Rensen PC. Inhibition of the central melanocortin system decreases brown adipose tissue activity. *J Lipid Res*. 2014;**55**(10):2022-2032.

40. Nogueiras R, Wiedmer P, Perez-Tilve D, Veyrat-Durebex C, Keogh JM, Sutton GM, Pfluger PT, Castaneda TR, Neschen S, Hofmann SM, Howles PN, Morgan DA, Benoit SC, Szanto I, Schrott B, Schurmann A, Joost HG, Hammond C, Hui DY, Woods SC, Rahmouni K, Butler AA, Farooqi IS, O'Rahilly S, Rohner-

721 Jeanrenaud F and Tschop MH. The central melanocortin system directly controls
722 peripheral lipid metabolism. *J Clin Invest*. 2007;**117**(11):3475-3488.
723 41. Ren H, Cook JR, Kon N and Accili D. Gpr17 in AgRP Neurons Regulates
724 Feeding and Sensitivity to Insulin and Leptin. *Diabetes*. 2015;**64**(11):3670-3679.
725 42. Sun Y, Liu S, Ferguson S, Wang L, Klepcyk P, Yun JS and Friedman JE.
726 Phosphoenolpyruvate carboxykinase overexpression selectively attenuates
727 insulin signaling and hepatic insulin sensitivity in transgenic mice. *J Biol Chem*.
728 2002;**277**(26):23301-23307.
729 43. Buettner C, Pocai A, Muse ED, Etgen AM, Myers MG, Jr. and Rossetti L.
730 Critical role of STAT3 in leptin's metabolic actions. *Cell Metab*. 2006;**4**(1):49-60.
731
732
733 **Figure Legends:**
734 **Figure 1:** (a) Schematic representation of AgRP gene deletion by CRISPR-Cas9.
735 (b) Genotyping of founders. Most pups display evidence of some cut and repair
736 activity, with 10/18 showing a large fragment deletion (indicated by red
737 numbering). Asterisks indicated animals taken forward for full sequencing. (c)
738 Summary of alignments of products against WT sequence. Blue bars indicate
739 alignment, white bars are loss of alignment/deletion. (d) Sequencing of founder
740 lines, with specific deletions indicated. Line 2 and 5 are perfect HDR, line 7 and
741 17 have deletions DNA between g335 and g193, and line 10 deletion between
742 g335 and g193
743
744 **Figure 2:** Food intake and leptin increase with 1 day treatment, but body weight
745 and fat pad mass increase later (a) Food intake is increased after 1, 2, and 3 days

and 3 weeks Cort treatment (day 1; n=23-24, day 2; n=15, day 3; n=8, 3 week; n=7-8). (b) Percentage body weight change (day 1; n=23, day 2; n=15, day 3; n=8, 3 week; n=7-8) and (c) mesenteric, inguinal and epididymal fat pad mass are increased after 3 weeks Cort treatment (n=7-8) (d) H&E staining of epididymal adipose tissue demonstrating larger adipocyte size after 3 weeks Cort treatment. Scale bar 100μm (n=4, 3 sections per slide). (e) Gastrocnemius muscle weight after 1, 2 and 3 days and 3 weeks Cort treatment (n=7-8). (f) Circulating leptin is increased after 1 day and is further increased after 3 weeks Cort treatment (n=6-8). (g) *Lep* (leptin) mRNA expression is increased after 1 day Cort treatment (n=6-8). White bars = vehicle, black bars = 75μg/ml corticosterone (Cort) treated. **P*<0.05, ***P*<0.01, ****P*<0.001. (a-e) Unpaired student's t-test. (f) 2-way ANOVA with Fisher's LSD post-test. (g) Unpaired Mann-Whitney t-test.

Figure 3: Impact of Cort treatment on BAT mass and RER (a) Brown adipose tissue (BAT) mass is increased from day 1 of Cort treatment (n=7-8). (b) Representative image of H&E staining of BAT after 2 days and 4 weeks Cort treatment. Scale bar = 100μm (n=4, 3 sections per slide). (c) Decreased thermogenic genes after 2 days Cort treatment (n=7-8). (d) UCP-1 protein expression is unchanged after 2 days and decreased after 4 weeks Cort treatment (n=5-6). (e) Decreased thermogenic genes in BAT after 3 weeks Cort treatment (n=7-8). (f) ANCOVA analysis showing no change in energy expenditure on days 1-3 or days 12-14 of Cort treatment (cohort 2, n=7). (g) Respiratory exchange ratio (RER) is increased during the day on days 1-3 and days 12-14 of Cort treatment in cohort 2 (n=7). White bars = vehicle and black bars = 75μg/ml corticosterone (Cort) treated. **P*<0.05, ***P*<0.01, ****P*<0.001. (a,

d) Unpaired Student's t-tests. (c, e) Unpaired Mann-Whitney t-tests. (f) ANCOVA analysis. (g) 2-way ANOVA with Fisher's LSD post-test.

Figure 4: Effect of Cort treatment on hyperglycaemia and insulin resistance (a) Circulating insulin is increased after 1 day and is further increased after 3 weeks Cort treatment (n=6-8). (b) Cort decreases epididymal adipose tissue, liver and skeletal muscle *Irs1* after 2 days Cort (n=7-8). (c) Epididymal adipose, liver, brown adipose and skeletal muscle *Irs1* are decreased after 3 weeks Cort (n=7-8). (d) Oil red O staining in liver after 2 days and 3 weeks Cort treatment. Scale bar = 50μm (n=4, 3 sections per mouse). (e) HOMA-IR is increased after 3 weeks Cort treatment in a separate cohort of mice (cohort 3, n=7-8). (f) Fed glucose is increased after 3 weeks Cort treatment (n=7-8). (g) Genes associated with gluconeogenesis are not increased after 2 days (n=7-8) and (h) but are increased after 3 weeks Cort treatment (n=7-8). White bars = vehicle and black bars = 75μg/ml corticosterone (Cort) treated. *P<0.05, **P<0.01, ***P<0.001. (a) Analysed by 4PL data logged to normalise. 2-way ANOVA with Fisher's LSD post-test. (b, c, g, h) Unpaired Mann-Whitney t-test. (e) Unpaired student's t-test (f) 2-way ANOVA with Fisher's LSD post-test

Figure 5: Cort treatment increases *Agrp* mRNA expression (a) Hypothalamic analysis of genes involved in energy balance after 1, 2 or 3 days or (c) 3 weeks Cort treatment. n=7-8. White bars = vehicle, black bars = 75μg/ml corticosterone (Cort) treated. *P<0.05, **P<0.01, ***P<0.001. Unpaired Mann-Whitney t-test

Figure 6: Loss of AgRP partially protects from Cort-induced hyperphagia (a) Representative colourimetric *in situ* hybridisation from AgRP$^{+/+}$ and AgRP $^{-/-}$ mice (n=3). (b) *Agrp* mRNA absent in AgRP$^{-/-}$ mice (n=9-10). (c) Twice weekly food intake over 3 weeks Cort treatment (n=7-10). Hypothalamic analysis of genes involved in (d) energy balance (n=7-10) and (e) Glucocorticoid responsive genes after 3 weeks Cort treatment in AgRP$^{+/+}$ and AgRP $^{-/-}$ mice (n=7-10). **P*<0.05, ***P*<0.01, ****P*<0.001. (f) Percent body weight change over 3 week Cort administration. (g) epididymal, mesenteric, inguinal, and brown adipose tissue mass after 3 weeks Cort treatment. White bars and symbols = vehicle AgRP$^{+/+}$, grey bars and symbols = vehicle AgRP$^{-/-}$, black bars and symbols = 75µg/ml corticosterone (Cort) AgRP$^{+/+}$, grey-hatched and symbols = 75µg/ml Cort AgRP $^{-/-}$ treated. * Vehicle AgRP$^{+/+}$ vs Cort AgRP$^{+/+}$; > Vehicle AgRP $^{-/-}$ vs Cort AgRP $^{-/-}$; + Cort AgRP$^{+/+}$ vs Cort AgRP$^{-/-}$. (b, d, e) Kruskill Wallis t test with Dunn's multiple comparison test (c, f) 2-way ANOVA, Tukey's multiple comparison test (g) One-way ANOVA, Tukey's multiple comparison

Figure 7: Loss of AgRP does not protect mice from Cort-induced insulin resistance or hyperglycaemia (a) Circulating insulin after 3 weeks Cort treatment is increased in AgRP$^{+/+}$ and AgRP $^{-/-}$ mice (n=8-10). (b) Hepatic *Irs1*, *P85a* and *P110b* mRNA expression (n=8-10). (c) Liver mass is not different between AgRP$^{+/+}$ and AgRP $^{-/-}$ mice (n=7-10). (d) Oil red O staining in liver after 3 weeks Cort treatment. Scale bar = 100µm (n=3-4, 6-9 sections per mouse). (e) Fed glucose levels (n=7-10) and (f) hepatic gluconeogenic genes (n=8-10) in AgRP$^{+/+}$ and AgRP $^{-/-}$ mice. **P*<0.05, ***P*<0.01, ****P*<0.001. (a) 4PL analysis, One way

819 ANOVA, Tukey's multiple comparison (c, e) One way ANOVA, Tukey's multiple
820 comparison (b, f) Kruskill Wallis t test with Dunn's multiple comparison test
821
822 **Table 1:** Sequence information or reference numbers of the qRT-PCR assays
823 employed.
824

Sefton et al. Figure 1

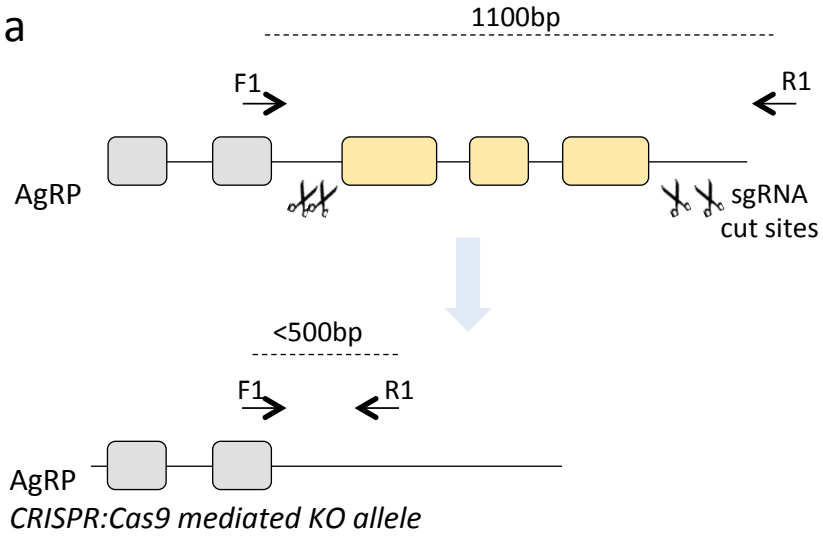

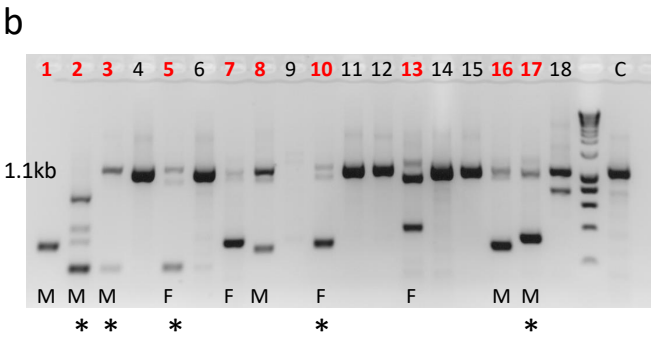

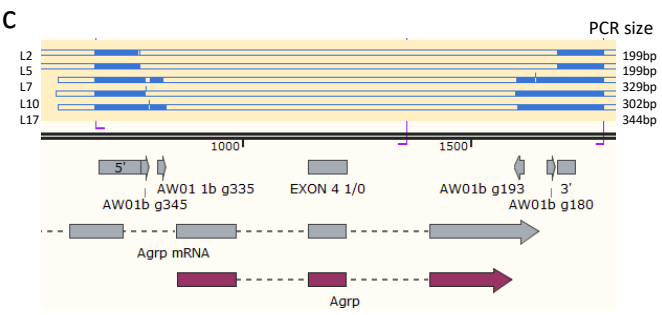

d

Line 2 GAATTGGGACTTTCT--------912bp deletion-----TTGTCGGGGCGTCGT ***HDR***

Line 5 GAATTGGGACTTTCT--------912bp deletion-----TTGTCGGGGCGTCGT ***HDR***

Line 7 TGGGAGCATCTCT–9bpDel-GGTAGGGTACCCTAAGGATGAGGAGAGA-773bpDel--TGTTGTTTG

Line 10 TGGGAGCATCTC--------809bp deletion-----GATGTTGTTTGGGCAAAG

Line 17 GGATGAGGAGAGACTAAATG--------769bp deletion-----TTGTTTGGGCAAAG

Sefton et al. Figure 2

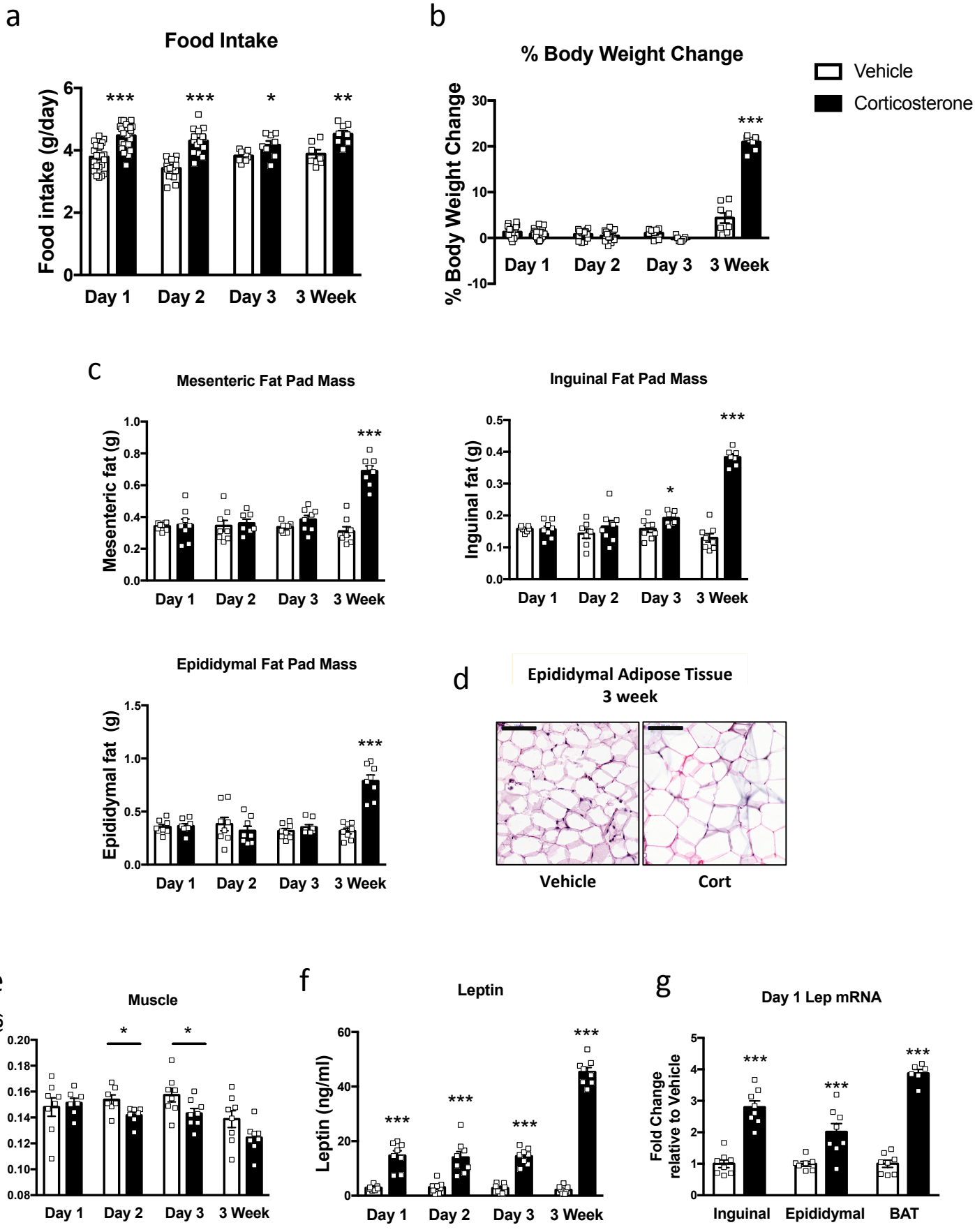

Sefton et al. Figure 3

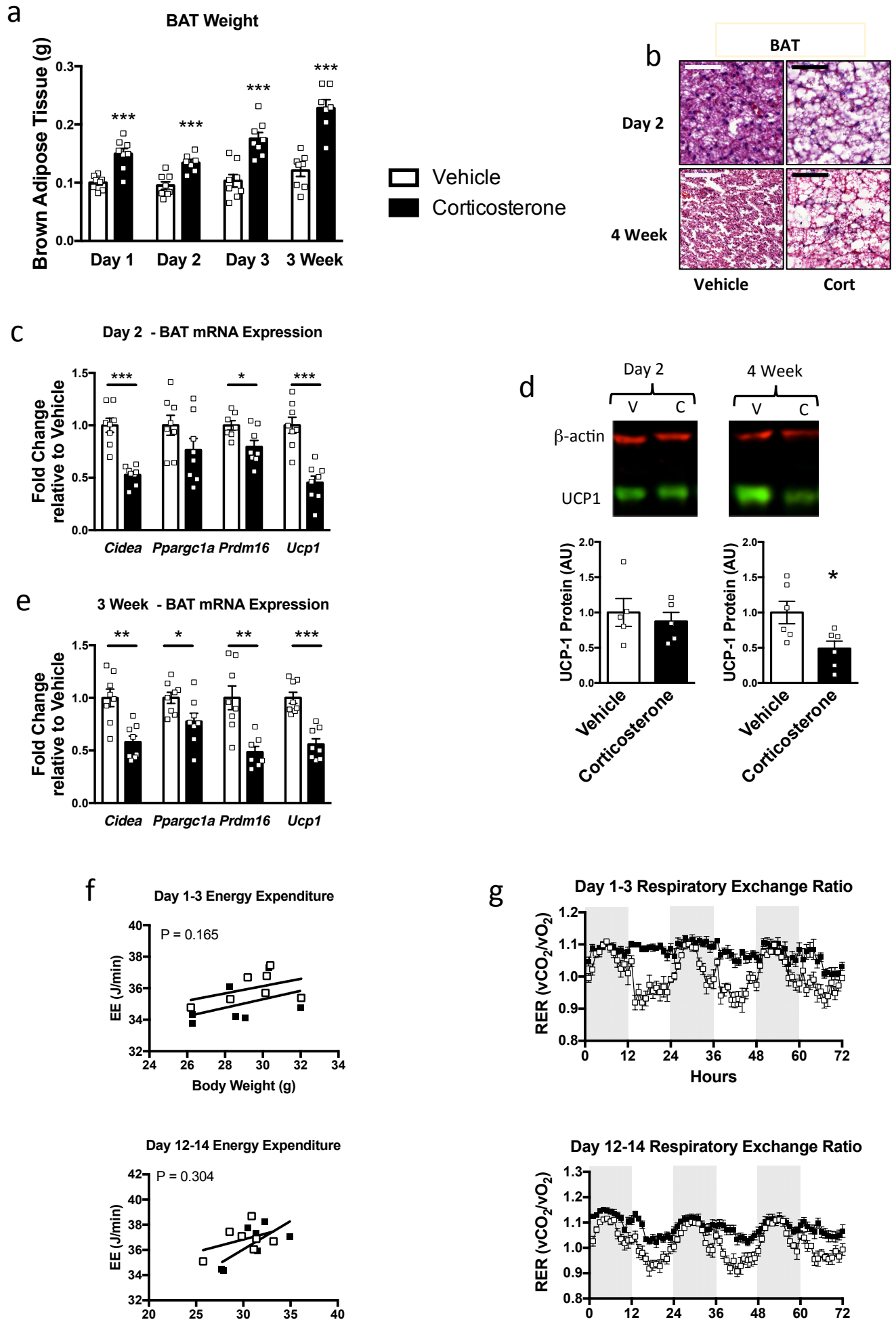

Sefton et al. Figure 4

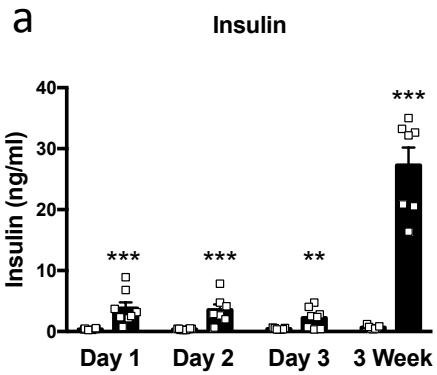

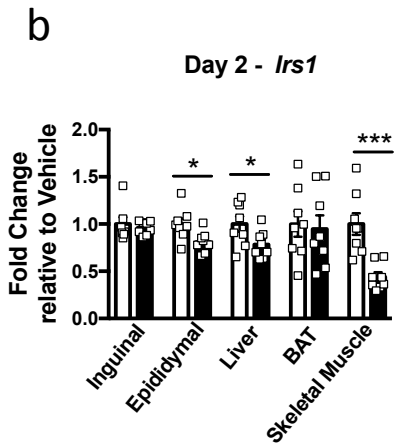

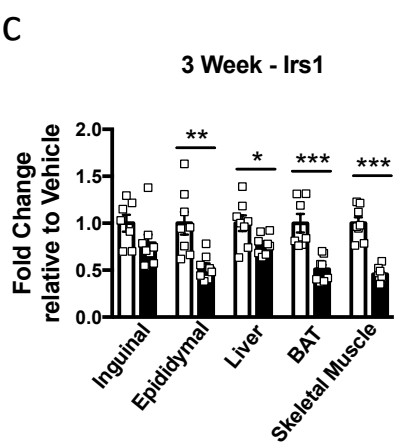

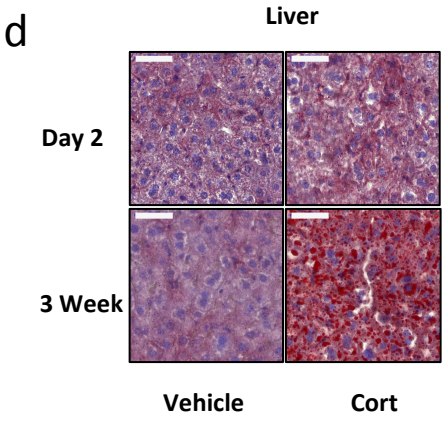

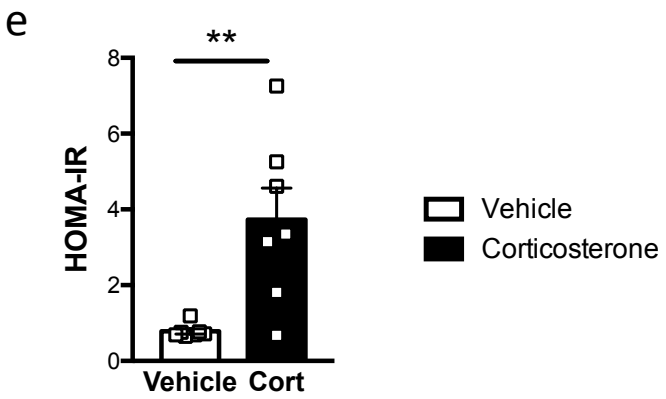

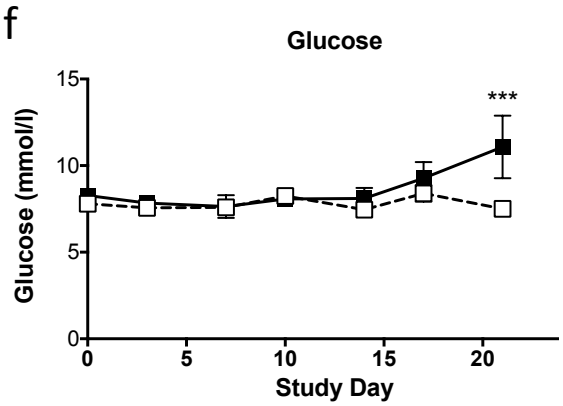

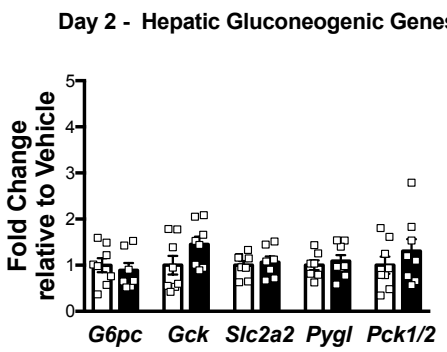

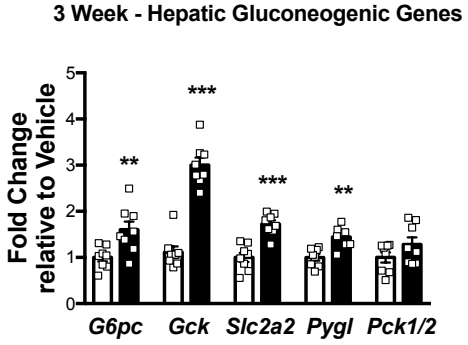

Sefton et al. Figure 5

a

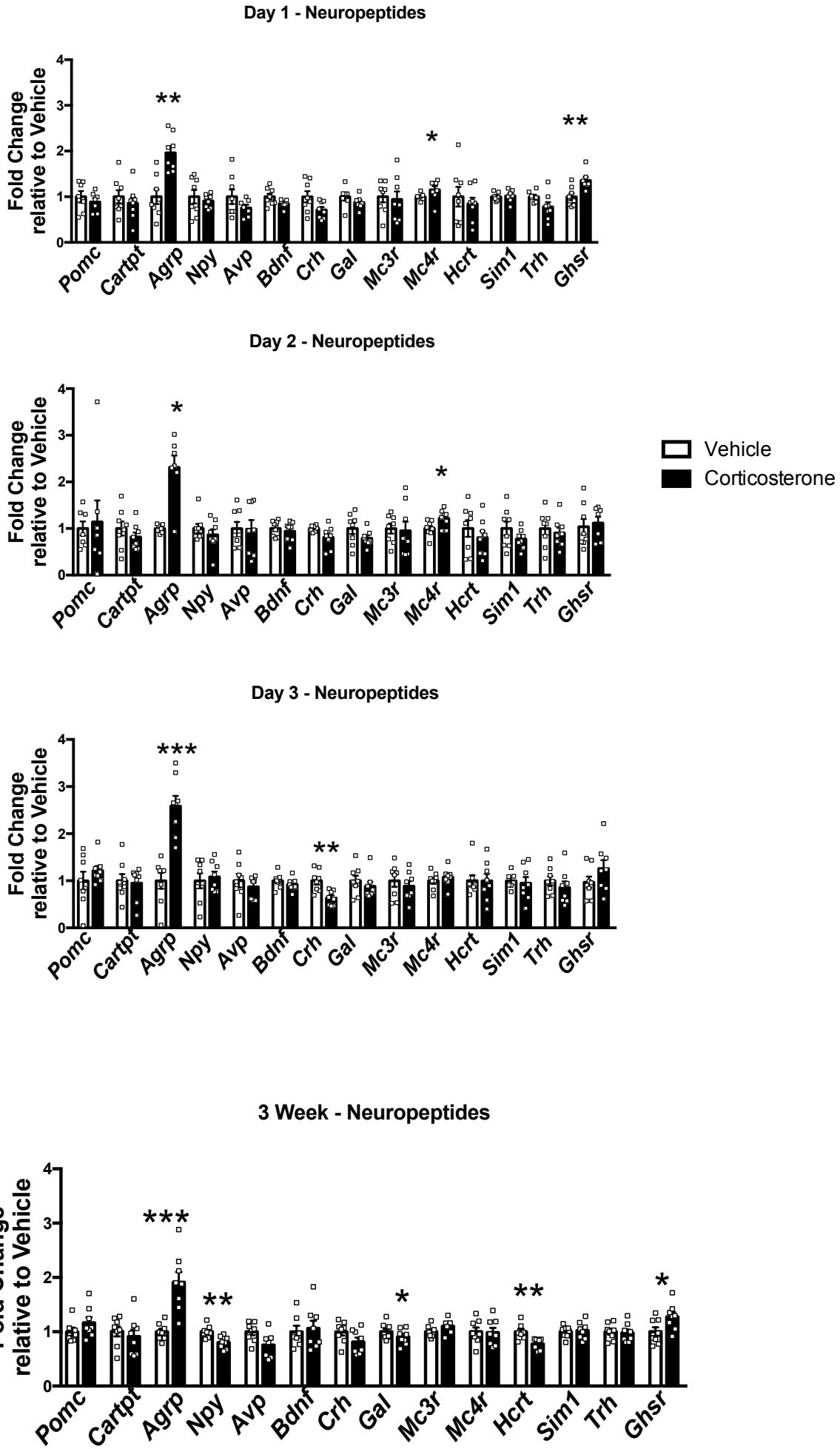

b

Sefton et al
Figure 6

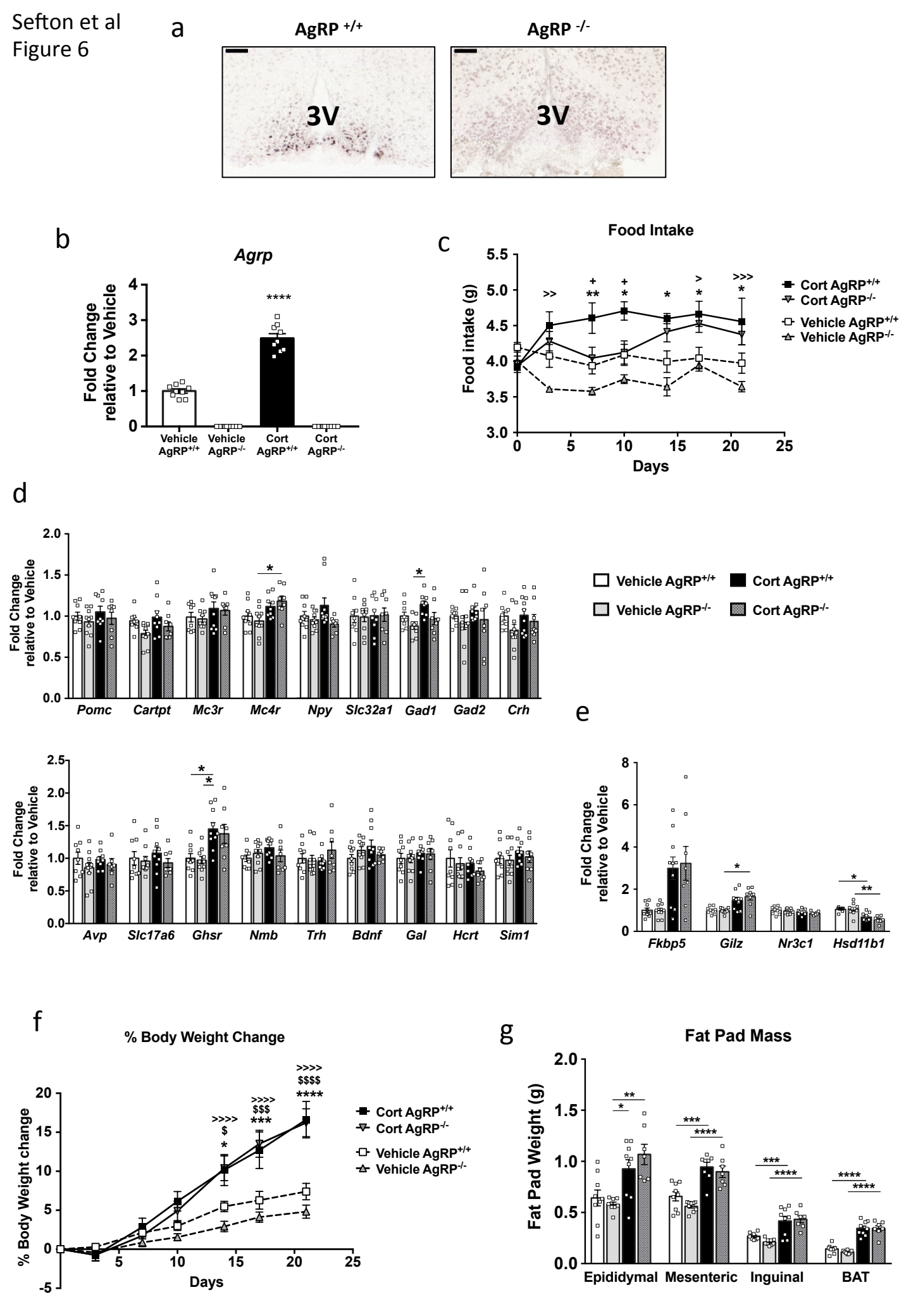

Sefton et al. Figure 7

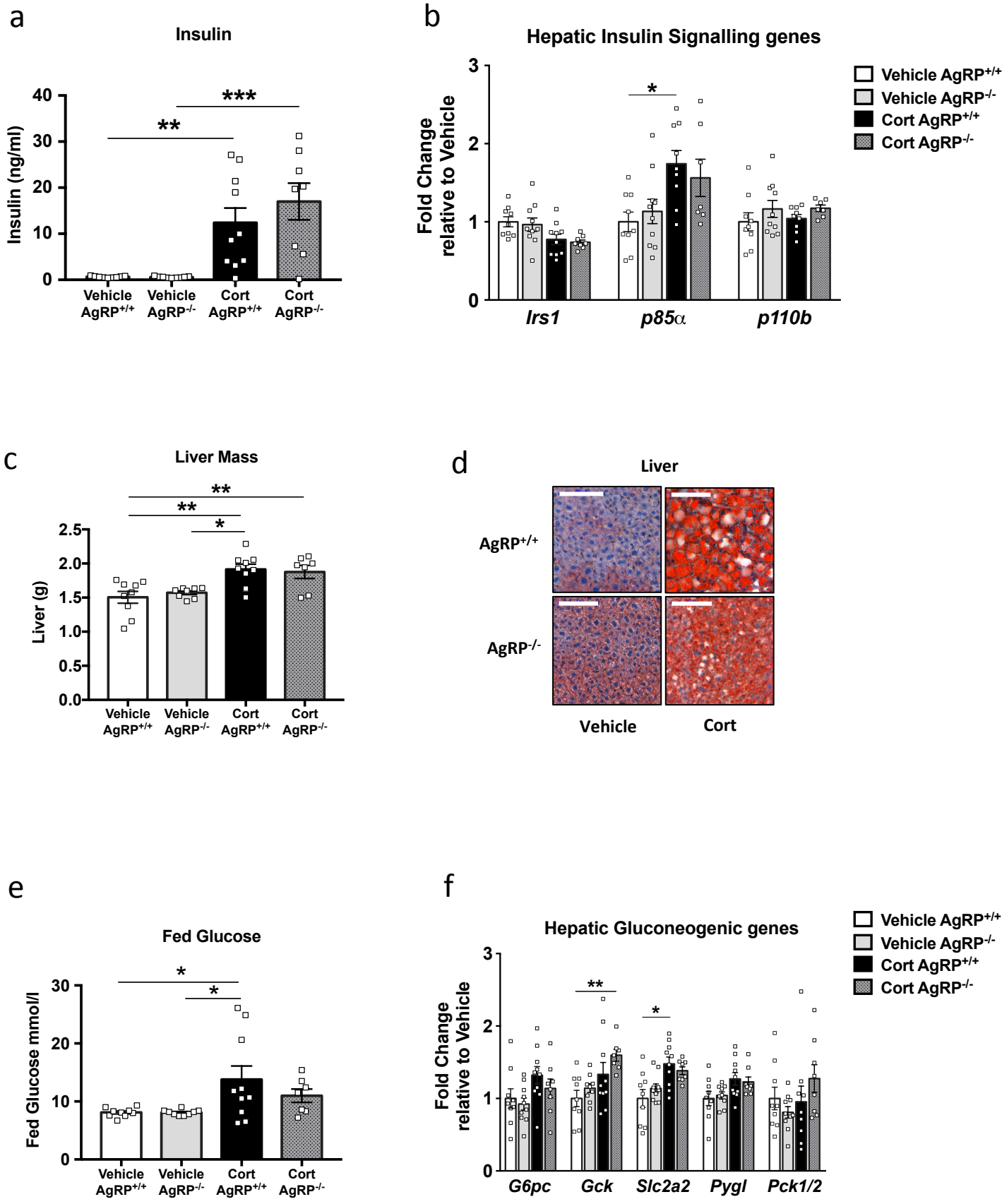

Sefton et al. Table 1

Gene	Forward 5'-3'	Reverse 5'-3'
Agrp	Mm00475829_g1	
Avp	Mm01271704_m1	
Bdnf	GCTCCGGGTTGGTATACTGG	CACCTGGTGGAACTTCTTTGC
Cartpt	Mm04210469_m	
Cidea	Mm00432554_m1	
Crh	Mm01293920_s1	
Fkbp5	AGCAACGGTAAAAGTCCACCT	TTCCCCAACAACGAACACCA
G6pc	GTGAGACCGGACCAGGAAGTC	ATCCCAACCACAAGATGACGTT
Gad1	Mm04207432_g1	
Gad2	Mm00484623_m1	
Gal	GCCCACATGCCATTGACAAC	GCACATCAACACTTCCTGGTC
Gck	AAGCTGCACCCGAGCTTCAA	GCTGCCCTCCTCTGATTCAA
Ghsr	AGATCGCGCAGATCAGTCAG	GTATTGATGCTCGACTTTGTCCA
Hcrt	TTTGGACCACTGCACTGAAGA	GGCCCAGGGAACCTTTGTAGA
Hprt	Mm03024075_m1	
Hsd11b1	Mm00476182_m1	
Irs1	CAAGACGCTCCAGTGAGGATT	TTTAGGTCTTCATTCTGCTGTGA
Klf4	AGAACAGCCACCCACACTTG	GTGGTAAGGTTTCTCGCCTGT
Lep	GCTCCAGAAGAAGAGGACCAA	GACTGAATTTCCAAAAGCCTGAA
Mc3r	TCAAGGAGATTCTCTGCGGC	ACACCCTTTTACGTCCCGTC
Mc4r	GGGTCGGAAACCATCGTCAT	CTGCAAATGGATGCGAGCAA
Nmb	CCTGCTCTTCGCATTGTTCG	AAGTGACCGGTCGCCCA
Npy	ATGCTAGGTAACAAGCGAATGG	TGTCGCAGAGCGGAGTAGTAT
Nr3c1	AGCTCCCCCTGGTAGAGAC	GGTGAAGACGCAGAAACCTTG
PCK1	CCTAGTGCCTGTGGGAAGAC	AAGTTGCCTTGGGCATCAAAC
Pomc	ATGCCGAGATTCTGCTACAGT	TCCAGCGAGAGGTCGAGTTT
Ppargc1a	AGCCGTGACCACTGACAACGAG	GCTGCATGGTTCTGAGTGCTAAG
Prdm16	GACATTCCAATCCCACCAGA	CACCTCTGTATCCGTCAGCA
Pygl	CCACTCGGACATCGTGAAGA	CCAATTTTCTCCGCTATCAAGTC
Sim1	GAGGAGGGAGAAAGAAAACAGTG	CCAAGCCCTTCTGGAAAGACC
Sla2a2	GATCGCTCCAACCACACTCA	CTGAGGCCAGCAATCTGACTA
Slc17a6	GGCTGGACACCAGTCTTTACAA	TTCTTCAGCACCCTGTAGATCTGT
Slc32a1	GGGTCACGACAAACCCAAGA	GCACGAACATGCCCTGAATG
Tbp	GGGAGAATCATGGACCAGAA	GATGGGAATTCCAGGAGTCA
Trh	CCTTGGTGCTGCCTTAGATTCC	CCCTCTCTTCGGCTTCAACG
Tsc22d3	GCAGGCCATGGACCTCGTGAAG	TCAGGAGGGTGTTCTCGCGCT
Ucp1	ACTGCCACACCTCCAGTCATT	CTTTGCCTCACTCAGG ATTGG
p110β	GCGCGGGGCAGTTCATCTTCTAA	GAGGCATGATAGGGCGGAAGCA
p85α	GCCAAGGAAACTGTCGCACACA	GGGGCAGTGCTGGTGGATCCAT